International Scientific Conference 20 UNITECH 26

INTERNATIONAL SCIENTIFIC CONFERENCE
19-21 November 2026
GABROVO

PID-BASED POSITION CONTROL AND DYNAMIC PERFORMANCE ANALYSIS OF A SINGLE-DEGREE-OF-FREEDOM VEHICLE SUSPENSION MODEL

Hilmi Kuşçu[1*], Ali Riza Motorcu[2]

[1]Trakya University, Faculty of Engineering, Department of Mechanical Engineering, Ahmet Karadeniz Campus, Edirne, Türkiye
[2]Canakkale Onsekiz Mart University, Faculty of Engineering, Department of Industrial Engineering, Terzioglu Campus, 17100, Canakkale, Türkiye

……
**Corresponding author: hilmi@trakya.edu.tr*

Abstract
Accurate displacement regulation in vehicle suspension models is important for limiting excessive motion and improving the dynamic response of mechanical systems subjected to transient excitations. This study investigates PID-based position control of a single-degree-of-freedom vehicle suspension model represented by a linear mass-spring-damper system. The governing equation is derived from Newton's second law, and the force-to-displacement transfer function is formulated using the physical parameters of the system. The model is characterized by a mass of 1 kg, a viscous damping coefficient of 3 N·s/m, and a stiffness of 2 N/m. A unity-feedback PID controller is designed to achieve a settling time below 0.6 s, overshoot below 10%, and zero steady-state tracking error. The controller gains are selected as K_p=160, K_i=220, and K_d=34. Numerical analysis yields approximately 3.74% overshoot and a 2% settling time of approximately 0.47 s. Closed-loop pole analysis confirms asymptotic stability. The study provides a transparent benchmark framework connecting the physical suspension model, controller design, transient-response evaluation, and stability assessment.

Keywords: vehicle suspension, PID control, position control, mass-spring-damper system, dynamic response.

1. INTRODUCTION

Vehicle suspension systems play an essential role in isolating the vehicle body from road-induced disturbances while maintaining adequate tire-road contact, vehicle stability, and ride quality. Suspension-control problems are commonly investigated using simplified quarter-car representations because these models provide a useful compromise between physical interpretability and dynamic fidelity [1, 2].

Proportional-integral-derivative (PID) control remains widely employed in suspension-control studies because of its simple structure, straightforward implementation, and ability to modify transient and steady-state characteristics [2–4].

Previous investigations have demonstrated that PID-based controllers can improve vehicle-body displacement and suspension response, while variations in suspension parameters can significantly affect overshoot and settling time [3, 4].

Recent research has increasingly focused on optimization-assisted and intelligent PID tuning. Pareto-based multiobjective optimization has been applied to quarter-vehicle active suspension systems to simultaneously consider suspension deflection, tire deflection, sprung-mass acceleration, and stability [5]. Fuzzy-PID controllers optimized using metaheuristic algorithms have also been investigated for semi-active quarter-car suspension systems [6].

This is an open access article licensed under Creative Commons Attribution 4.0 International
Print ISSN: 1313-230X, Online ISSN: 3033-1404

More recently, learning-assisted PID strategies and hybrid optimization techniques have been introduced to improve controller adaptability and robustness [7, 8]. Wu and Su employed a Q-learning-assisted neural-network PID controller for a quarter-car active suspension model [7], whereas Ram et al. combined system identification with hybrid optimization for robust PID tuning [8].

Advanced controller structures, including PID with derivative filtering and fractional-order controllers, have also been optimized using recent metaheuristic algorithms for quarter-car suspension applications [9]. These developments demonstrate the increasing sophistication of suspension-control methods; however, they also introduce additional controller parameters and computational complexity.

In contrast, the present study intentionally employs a reduced SDOF representation and a conventional PID controller. The objective is to establish a transparent benchmark in which the relationship among the physical parameters, transfer-function model, controller gains, transient-response characteristics, and closed-loop pole locations can be directly traced.

2. MATHEMATICAL MODEL OF THE SINGLE-DEGREE-OF-FREEDOM VEHICLE SUSPENSION SYSTEM

The investigated vehicle suspension system is represented by a single-degree-of-freedom (SDOF) mass-spring-damper model, as illustrated in Fig. 1. The physical representation of the wheel suspension system is shown in Fig. 1(a), where the vehicle body, suspension spring, damper, and wheel assembly are identified. For mathematical analysis, the physical system is reduced to the simplified mass-spring-damper representation shown in Fig. 1(b).

In this model, the vehicle body is represented by an equivalent mass *m*, the elastic behavior of the suspension is characterized by the spring stiffness *k*, and energy dissipation is represented by the viscous damping coefficient *b*. The vertical displacement of the equivalent mass is denoted by *x(t)*, while *F(t)* represents the externally applied force.

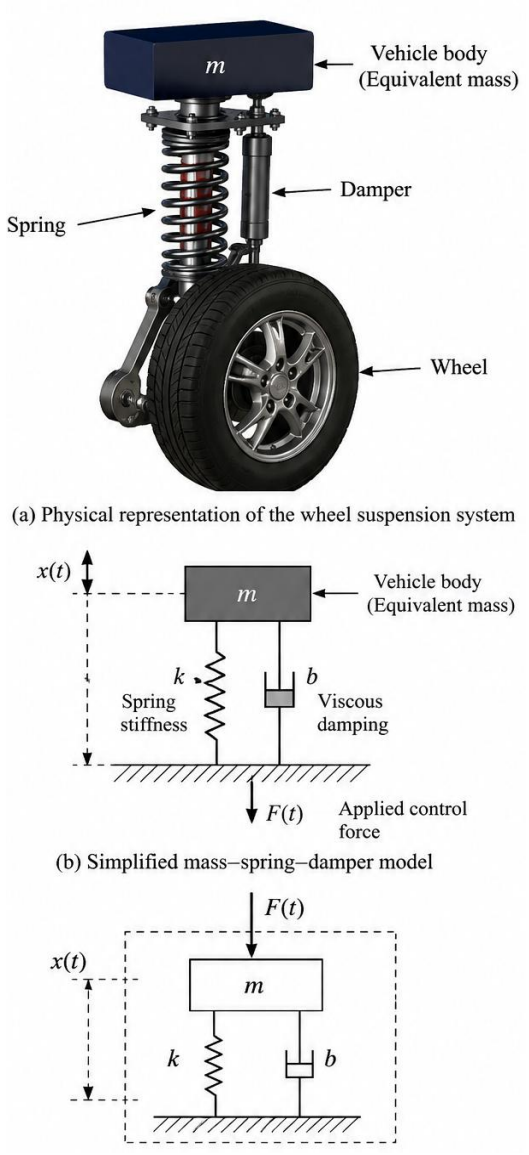


Fig. 1. *Single-degree-of-freedom vehicle suspension model: (a) physical representation of the wheel suspension system, (b) simplified mass-spring-damper representation, and (c) equivalent SDOF model used for mathematical analysis.*

The dynamic behavior of the simplified mechanical system is obtained by applying Newton's second law to the equivalent mass. The resulting governing equation of motion is given in Eq. (1).

$$m\,\ddot{x}(t) + b\,\dot{x}(t) + k\,x(t) = F(t) \quad (1)$$

In Eq. (1), $m\ddot{x}(t)$ represents the inertial force, $b\dot{x}(t)$ represents the viscous damping force, and $kx(t)$ represents the elastic restoring force generated by the spring. Accordingly, Eq. (1) establishes the relationship between the externally applied force $F(t)$ and the resulting displacement $x(t)$ of the equivalent mass.

For transfer-function analysis, zero initial conditions are assumed and the Laplace transform is applied to Eq. (1). The resulting algebraic relationship between the input force and the displacement in the Laplace domain is presented in Eq. (2).

$$(ms^2 + bs + k)X(s) = F(s) \quad (2)$$

Here, $X(s)$ and $F(s)$ denote the Laplace transforms of the displacement $x(t)$ and applied force $F(t)$, respectively, while \(s\) is the complex Laplace variable. Based on Eq. (2), the force-to-displacement transfer function of the mechanical system is defined by Eq. (3).

$$G(s) = \frac{X(s)}{F(s)} = \frac{1}{ms^2+bs+k} \quad (3)$$

Table 1. *Mechanical parameters of the SDOF vehicle suspension model.*

Parameter	Description	Value
m	Equivalent mass	1 kg
b	Viscous damping coefficient	3 N·s/m
k	Spring stiffness	2 N/m

As listed in Table 1, the numerical model employs an equivalent mass of 1 kg, a viscous damping coefficient of 3 N·s/m, and a spring stiffness of 2 N/m. Substitution of these parameter values into Eq. (3) yields the numerical plant transfer function given in Eq. (4).

$$G(s) = \frac{1}{s^2+3s+2} = \frac{1}{(s+1)(s+2)} \quad (4)$$

As indicated by Eq. (4), the characteristic polynomial of the uncontrolled mechanical system is s^2+3s+2. The roots of this characteristic polynomial, which correspond to the open-loop poles of the system, are given in Eq. (5).

$$p_1 = -1, p_2 = -2 \quad (5)$$

According to Eq. (5), both open-loop poles have negative real values and are therefore located in the open left half of the complex s-plane. Consequently, the uncontrolled mechanical system is asymptotically stable.

3. PID CONTROLLER DESIGN AND PERFORMANCE CRITERIA

A unity negative-feedback control architecture is employed to regulate the displacement of the single-degree-of-freedom vehicle suspension model. In this configuration, the desired position $r(t)$ is continuously compared with the measured displacement $x(t)$. The tracking error used as the input to the PID controller is defined in Eq. (6).

$$e(t) = r(t) - x(t) \quad (6)$$

In Eq. (6), $r(t)$ denotes the reference position, $x(t)$ represents the actual displacement of the controlled mass, and $e(t)$ is the instantaneous position-tracking error. The objective of the controller is therefore to reduce $e(t)$ toward zero while satisfying the prescribed transient-response requirements.

The closed-loop PID position-control architecture used in this study is illustrated in Fig. 2. The PID controller generates the control action from the proportional, integral, and derivative components of the tracking error. In the Laplace domain, the ideal parallel-form PID controller is expressed by Eq. (7).

$$C(s) = K_p + \frac{K_i}{s} + K_d s \quad (7)$$

In Eq. (7), K_p is the proportional gain, K_i is the integral gain, and K_d is the derivative

gain. The proportional component responds directly to the instantaneous error, the integral component contributes to the elimination of steady-state error, and the derivative component provides an anticipatory action based on the rate of change of the error.

For subsequent transfer-function operations, Eq. (7) can equivalently be expressed as the rational function given in Eq. (8).

$$C(s) = \frac{K_d s^2 + K_p s + K_i}{s} \tag{8}$$

The controller parameters are selected to satisfy three principal position-control requirements: a 2% settling time below 0.6 s, a maximum overshoot below 10%, and zero steady-state tracking error. These performance objectives were adopted as the design criteria for the present analysis.

The controller gains were determined through numerical tuning of the plant model given in Eq. (4) by iteratively evaluating the closed-loop unit-step response against the prescribed settling-time, overshoot, and steady-state-error requirements. The resulting gain set was K_p=160, K_i=220, and K_d=34. Substitution of these gains into Eq. (8) gives the numerical PID controller transfer function presented in Eq. (9).

$$C(s) = \frac{34s^2 + 160s + 220}{s} \tag{9}$$

Equation (9) therefore represents the specific PID controller used throughout the subsequent numerical and stability analyses.

For a unity negative-feedback configuration, the relationship between the controller *C(s)*, the plant *G(s)*, and the resulting closed-loop system is defined by Eq. (10).

$$T(s) = \frac{C(s)G(s)}{1 + C(s)G(s)} \tag{10}$$

In Eq. (10), *T(s)* denotes the closed-loop transfer function from the reference position to the controlled displacement. Substituting the plant transfer function given in Eq. (4) and the PID controller given in Eq. (9) into Eq. (10) results in the closed-loop transfer function presented in Eq. (11).

$$T(s) = \frac{34s^2 + 160s + 220}{s^3 + 37s^2 + 162s + 220} \tag{11}$$

Equation (11) constitutes the mathematical basis for the subsequent transient-response and closed-loop stability analyses. Its denominator, $s^3+37s^2+162s+220$ is the characteristic polynomial of the PID-controlled closed-loop system.

4. MATLAB-BASED NUMERICAL IMPLEMENTATION

The mathematical model described by Eqs. (4), (9), and (11) was implemented in MATLAB for numerical evaluation of the closed-loop position-control performance. The plant was represented using the transfer function in Eq. (4), while the proportional, integral, and derivative gains were assigned according to the controller defined in Eq. (9). Unity negative feedback was then applied according to the closed-loop formulation given in Eq. (10).

The numerical implementation was used to determine the unit-step position response, transient-response characteristics, steady-state tracking behavior, and closed-loop pole locations. In this manner, all numerical results presented in the following sections are derived from the same mathematical model and controller parameters, ensuring consistency between the analytical formulation and numerical analysis.

5. RESULTS AND DISCUSSION

5.1. Position Step Response

The transient position-control performance was evaluated by applying a unit-step reference input to the closed-loop system defined in Eq. (11). The resulting response is presented in Fig. 3.

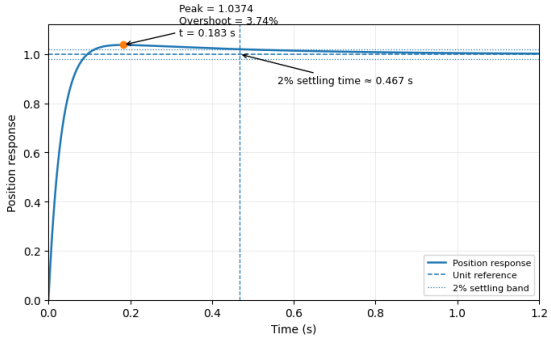


Fig. 3. *Unit-step position response of the PID-controlled single-degree-of-freedom vehicle suspension system.*

The unit-step analysis yielded a maximum overshoot of approximately 3.74% and a 2% settling time of approximately 0.47 s. Both values satisfy the specified design requirements of M_p<10% and T_s<0.6 s. Furthermore, the integral component of the PID controller enables the output displacement to converge to the unit reference, resulting in zero steady-state tracking error for the ideal model. Thus, the transient response demonstrates that the selected PID gains provide the desired compromise between rapid convergence and limited overshoot for the investigated SDOF mechanical system.

5.2. Quantitative Performance Evaluation

The principal transient and steady-state performance indicators obtained from the unit-step response in Fig. 3 are summarized in Table 2. The prescribed design limits are also included to provide a direct quantitative comparison with the achieved closed-loop performance.

Table 2. *Performance of the PID-controlled system.*

Performance indicator	Requirement	Result
Maximum overshoot, M_p	< 10%	**3.74%**
Settling time, T_s (2%)	< 0.60 s	**0.467 s**
Steady-state error, e_{ss}	0	**≈ 0**
Closed-loop stability	Stable	**Stable**

As shown in Table 2, the maximum overshoot is 3.74%, which remains well below the specified 10% limit. The 2% settling time is approximately 0.467 s and therefore satisfies the requirement of less than 0.60 s. In addition, the output converges to the unit reference with approximately zero steady-state error. These results demonstrate that the selected PID gains satisfy all specified position-control performance requirements.

5.3. Stability Analysis

The stability of the PID-controlled system is evaluated using the characteristic polynomial obtained from the denominator of the closed-loop transfer function in Eq. (11). Accordingly, the closed-loop characteristic equation is expressed in Eq. (12).

$$s^3 + 37s^2 + 162s + 220 = 0 \qquad (12)$$

The roots of Eq. (12) determine the closed-loop pole locations and therefore provide a direct assessment of system stability. The calculated poles are presented in Eq. (13).

$$p_1 = -32.178,$$
$$p_{2,3} = -2.411 \pm j1.012 \qquad (13)$$

As shown in Eq. (13), all closed-loop poles have negative real parts. The corresponding pole locations are illustrated in Fig. 4. Since all poles are located in the open left half of the complex s-plane, the PID-controlled closed-loop system is asymptotically stable.

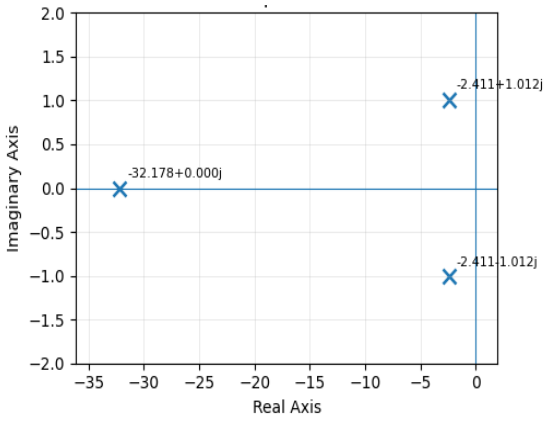


Fig. 4. *Pole locations of the PID-controlled closed-loop system.*

The complex-conjugate pole pair in Eq. (13) is associated with the oscillatory component of the transient response, whereas the real pole located farther to the left represents a considerably faster dynamic mode. This pole configuration is consistent with the stable and well-damped unit-step response observed in Fig. 3.

5.4. Relation to Recent Studies

Recent studies demonstrate a clear progression from conventional PID-based suspension control toward optimization-assisted and intelligent controller-tuning strategies. Conventional PID implementations using quarter-car models have demonstrated the capability of PID control to improve suspension dynamic response [2–4]. More advanced investigations have employed multiobjective and metaheuristic optimization to tune PID parameters while considering several suspension-performance criteria simultaneously [5, 6].

Learning-assisted and hybrid optimization techniques have further extended this approach. Wu and Su [7] employed Q-learning and a neural-network-based PID structure for quarter-car active suspension control, while Ram et al. [8] combined system identification with conventional and hybrid optimization algorithms for robust PID tuning. Recent work has also considered PIDN and fractional-order controller structures optimized using multiple metaheuristic algorithms [9].

Unlike these higher-order and optimization-intensive approaches, the present study intentionally employs a reduced SDOF representation. The purpose is not to reproduce the complete dynamics of an automotive suspension but to establish an analytically transparent benchmark in which the relationships among the physical parameters, plant transfer function, PID gains, transient-response characteristics, and closed-loop poles can be directly traced. For the investigated model, the obtained settling time of approximately 0.467 s, maximum overshoot of 3.74%, zero steady-state error, and stable closed-loop pole configuration demonstrate that the selected PID controller satisfies the specified design objectives. The simplified formulation therefore provides a suitable foundation for subsequent investigations involving higher-order vehicle models, road disturbances, actuator dynamics, parameter uncertainty, and advanced PID-tuning strategies.

6. CONCLUSION

This study presented a PID-based position-control approach for a simplified single-degree-of-freedom vehicle suspension model. The mechanical system was formulated using an equivalent mass, linear spring, and viscous damper, and a physically consistent force-to-displacement transfer function was derived from the governing equation of motion. A PID controller was subsequently incorporated into a unity negative-feedback configuration, and the resulting closed-loop system was evaluated in terms of transient response, steady-state tracking, and pole locations.

For the investigated system parameters, the selected gains of K_p=160, K_i=220, and K_d=34 resulted in a maximum overshoot of approximately 3.74% and a 2% settling time of approximately 0.467 s. The system also achieved zero steady-state error for the unit-step reference. Furthermore, all closed-loop poles were located in the open left half of the complex plane, confirming asymptotic stability. Consequently, the specified requirements of less than 10% overshoot and less than 0.6 s settling time were satisfied.

The principal contribution of the study is the establishment of a consistent and analytically traceable framework connecting the physical SDOF model, transfer-function formulation, PID controller design,

transient-response evaluation, and closed-loop stability analysis. Although the simplified model does not represent tire dynamics, road-profile excitation, actuator dynamics, or the additional degrees of freedom encountered in complete vehicle suspension models, it provides a useful benchmark for controller-development studies. Future work can extend the proposed framework to quarter-car models incorporating sprung and unsprung masses, road disturbances, parameter uncertainties, and optimization-based or adaptive PID tuning strategies.

REFERENCES

[1] Rao KD. Modeling, simulation and control of semi active suspension system for automobiles under MATLAB Simulink using PID controller. IFAC Proceedings Volumes 2014; 47(1):827-831. DOI: 10.3182/20140313-3-IN-3024.00094.

[2] Trang NV, Lan DNH. Modeling and simulation of PID controller-based active suspension system for a quarter car model. Journal of Technical Education Science 2022; 17(1):111-120. DOI: 10.54644/jte.68.2022.1126.

[3] Mohammed MH, Bash AM. PID controller of a car with quarter body active suspension system. Journal of Advanced Sciences and Engineering Technologies 2018; 2(1):1-12. DOI: 10.32441/jaset.02.01.01.

[4] Ferdinandus ARA, Sepang NG. Analysis of parameter changes in controlling the quarter-car active suspension with PID controller. Jurnal Teknik Elektro dan Komputer 2021; 10(3): 205-212.

[5] Gampa SR, Mangipudi SK, Jasthi K, Babu BM, Goli P, Das D, Balas, VE. Pareto optimality based PID controller design for vehicle active suspension system using grasshopper optimization algorithm. Journal of Electrical Systems and Information Technology 2022; 9:24. DOI: 10.1186/s43067-022-00065-y.

[6] Liu Y, As'arry A, Ahmed H, Hairuddin AA, Hassan MK, Zakaria MZ, Yang S. Online optimal tuning of fuzzy PID controller using grey wolf optimizer for quarter car semi-active suspension system. Advances in Mechanical Engineering 2024; 16(2):1-14. DOI: 10.1177/16878132231219620.

[7] Wu Y, Su D. Simulation analysis of quarter car active suspension control based on QBP-PID. Proceedings of the Institution of Mechanical Engineers, Part D: Journal of Automobile Engineering 2025; 239(9):4135-4143. DOI: 10.1177/09544070241265152.

[8] Ram SS, Kumar C, Saravanakumar R, Banjerdpongchai D. System identification and robust PID controller tuning of quarter car suspension system using hybrid optimization techniques. Scientific Reports 2025; 15:24195. DOI: 10.1038/s41598-025-10213-9.

[9] Özbilgin F, Mengi OÖ, Wadood A, Güven AF, Park H. Comparative optimization of PIDN and fractional order controllers for a quarter car active suspension system using recent metaheuristic algorithms. Scientific Reports 2025; 15:35222. DOI: 10.1038/s41598-025-19505-6.